IBRO Reports 9 (2020) 102–114

Contents lists available at ScienceDirect

IBRO Reports

journal homepage: www.elsevier.com/locate/ibror

Research Paper

Alpha-pinene and dizocilpine (MK-801) attenuate kindling development and astrocytosis in an experimental mouse model of epilepsy

Hiroshi Ueno[a,*], Atsumi Shimada[b], Shunsuke Suemitsu[c], Shinji Murakami[c], Naoya Kitamura[c], Kenta Wani[c], Yu Takahashi[c], Yosuke Matsumoto[d], Motoi Okamoto[e], Takeshi Ishihara[c]

[a] Department of Medical Technology, Kawasaki University of Medical Welfare, Okayama, 701-0193, Japan
[b] Division of Food and Nutrition, Nakamura Gakuen University Junior College, Fukuoka, 814-0198, Japan
[c] Department of Psychiatry, Kawasaki Medical School, Okayama, 701-0192, Japan
[d] Department of Neuropsychiatry, Graduate School of Medicine, Dentistry and Pharmaceutical Sciences, Okayama University, Okayama, 700-8558, Japan
[e] Department of Medical Technology, Graduate School of Health Sciences, Okayama University, Okayama, 700-8558, Japan

ARTICLE INFO

Keywords:
Epilepsy
Kindling
Pentylenetetrazol
Perineuronal nets
Wisteria floribunda

ABSTRACT

Understanding the molecular and cellular mechanisms involved during the onset of epilepsy is crucial for elucidating the overall mechanism of epileptogenesis and therapeutic strategies. Previous studies, using a pentylenetetrazole (PTZ)-induced kindling mouse model, showed that astrocyte activation and an increase in perineuronal nets (PNNs) and extracellular matrix (ECM) molecules occurred within the hippocampus. However, the mechanisms of initiation and suppression of these changes, remain unclear.

Herein, we analyzed the attenuation of astrocyte activation caused by dizocilpine (MK-801) administration, as well as the anticonvulsant effect of α-pinene on seizures and production of ECM molecules. Our results showed that MK-801 significantly reduced kindling acquisition, while α-pinene treatment prevented an increase in seizures incidences. Both MK-801 and α-pinene administration attenuated astrocyte activation by PTZ and significantly attenuated the increase in ECM molecules.

Our results indicate that astrocyte activation and an increase in ECM may contribute to epileptogenesis and suggest that MK-801 and α-pinene may prevent epileptic seizures by suppressing astrocyte activation and ECM molecule production.

1. Introduction

Epilepsy is a neurological disorder that manifests with rapid, recurrent seizures resulting from the synchronized discharging of brain neurons. At least 1 % of the world's population is affected by epilepsy (Fisher et al., 2005; WHO Factsheet, 2001). Despite treatment with currently available antiepileptic drugs (AEDs), 30 % of patients with epilepsy remain refractory to therapy (Schmidt and Löscher, 2005; Rahmati et al., 2013). Given the high proportion of patients who do not respond to the currently available treatments, identifying seizure mechanisms and searching for new therapeutic targets is essential. However, the pathophysiological processes leading to epilepsy remain poorly understood.

Kindling is a common functional model of temporal lobe epilepsy (Kandratavicius et al., 2014), and it references an initially small epileptic stimuli being repeated and amplified, much like the initial kindling of twigs to produce a large fire. Systemic administration of PTZ establishes systemic, tonic-clonic seizures and provides an excellent model for studying epileptogenesis in mice (Mandhane et al., 2007). PTZ-induced kindling is the most common animal model for studying seizure mechanisms and understanding the neurobiology of epilepsy. It has also been used for the examination of learning and memory problems caused by seizures and evaluation of new treatment effects. (Dhir, 2012; Pahuja et al., 2013; Atinga et al., 2015).

Despite treatment with AEDs, epilepsy remains challenging due to the side effects from these medications (Elger et al., 2004). Recent research has focused on the development of more effective AEDs with minimal or no side effects. Many monoterpenes, commonly present in

* Corresponding author at: Department of Medical Technology, Kawasaki University of Medical Welfare, 288, Matsushima, Kurashiki, Okayama, 701-0193, Japan.
E-mail addresses: dhe422007@s.okayama-u.ac.jp (H. Ueno), atsushimada@nakamura-u.ac.jp (A. Shimada), ssue@med.kawasaki-m.ac.jp (S. Suemitsu), muraka@med.kawasaki-m.ac.jp (S. Murakami), n-kitamura@med.kawasaki-m.ac.jp (N. Kitamura), k-wani@med.kawasaki-m.ac.jp (K. Wani), yuuu.takahashi@gmail.com (Y. Takahashi), ymatsumoto@cc.okayama-u.ac.jp (Y. Matsumoto), mokamoto@md.okayama-u.ac.jp (M. Okamoto), t-ishihara@med.kawasaki-m.ac.jp (T. Ishihara).

https://doi.org/10.1016/j.ibror.2020.07.007
Received 9 March 2020; Accepted 11 July 2020

essential oils, are known for their anticonvulsant properties (de Sousa et al., 2006; Zhu et al., 2014; Souto-Maior et al., 2017). The monoterpene, α-pinene, is an organic terpene compound found in coniferous oils, and is the primary monoterpene of pine trees (Simonsen and Ross, 1957). Essential oils, including α-pinene, have been used to treat various diseases (Mercier et al., 2009). α-pinene is widely used as a food flavoring ingredient (Pereira Limberger et al., 2007; Ana Cristina da Silva Rivas et al., 2012) and has been approved as a safe food additive by the U.S. Food and Drug Administration (FDA 2015). α-pinene has anti-inflammatory (Martin et al., 1993; Zhou et al., 2004), anti-depressive (Ahmad et al., 2013), anti-oxidative (Singh et al., 2006), anti-tumor (Eftekhar et al., 2004), and anti-nociceptive effects (Him et al., 2008). However, the antiepileptic effects of α-pinene remain unclear. We investigated the protective effects of α-pinene on status epilepticus in an experimental model of epilepsy and explored the potential molecular events involved in this effect.

The molecular mechanisms underlying kindling and the development of abnormal excitability in epilepsy are poorly understood. Studies have shown that changes in synaptic plasticity lead to epilepsy (Scharfman et al., 2002; Jarero-Basulto JJ et al., 2018). We have shown in previous studies that activation of astrocytes in the PTZ-induced kindling model may lead to increased ECM secretion (Ueno et al., 2019a, 2019b). Dizocilpine (MK-801), a noncompetitive N-methyl-D-aspartate (NMDA) antagonist, has been reported to significantly reduce glutamate-stimulated astrocyte activation (Chan et al., 1990). Since cultured astrocytes lack NMDA receptors, it is suggested that MK-801 suppressed astrocyte activation by a mechanism independent of the NMDA receptor. To elucidate the mechanism of ECM increase and astrocyte activation in kindling acquisition, we previously administered MK-801 and investigated the effects within a PTZ-induced kindling model.

ECM in the central nervous system (CNS) includes components such as hyaluronic acid, tenascin-R, glycoproteins, and chondroitin sulfate proteoglycans (CSPG) (Maeda, 2015). In the mature CNS, ECM molecules are distributed as neural granules or perineuronal nets (PNNs), which are concentrated meshwork structures (Maeda, 2015). In the cortex and hippocampus, PNNs mainly form around parvalbumin-positive GABAergic interneurons (Slaker et al., 2016). Although the exact function of PNNs is unknown, it is believed that they stabilize synaptic connectivity and regulate retention of synaptic plasticity (Frischknecht et al., 2009; Kalb and Hockfield, 1994; Pizzorusso et al., 2002). Some reports have suggested that plasticity is controlled by the aggrecan molecule, which is a component of PNNs (McRae et al., 2007; Ye and Miao, 2013; Ueno et al., 2017a, 2017b). The plant lectin, wisteria floribunda agglutinin (WFA), is commonly used to detect PNNs. WFA binds to N-acetylgalactosamine (Seeger et al., 1994; Schweizer et al., 1993; Brückner et al., 1993). The antibody Cat-315, which is specific for the aggrecan molecule, is also often used to detect PNNs. Cat-315 recognizes the human natural killer 1 carbohydrate epitope of aggrecan (Matthews et al., 2002; McRae et al., 2007; Dino et al., 2006). In this study, WFA lectin and Cat-315 were used to investigate the expression of PNNs and other ECM molecules.

We considered that α-pinene, which has been reported to have anticonvulsant activity, may also exhibit antiepileptic activity. We also speculated that MK-801, which suppresses astrocyte activation, may exhibit antiepileptic activity. This study aimed to investigate whether α-pinene and MK-801 had antiepileptic effects and could inhibit status epilepticus. Furthermore, we sought to clarify the effects of α-pinene and MK-801 on astrocyte activation and ECM molecule expression during kindling acquisition. The findings may lead to the development of new therapeutic agents to prevent epilepsy.

2. Methods

2.1. Animals

Eleven-week-old, male mice (C57BL/6 N) were used for all experiments. Mice were housed, five to a cage, under standard animal care conditions. All procedures related to animal maintenance and experimentation were approved by the Committee for Animal Experiments at the Kawasaki Medical School Advanced Research Center and conformed to the U.S. National Institutes of Health Guide for the Care and Use of Laboratory Animals (NIH Publication No. 80-23, revised in 1996). Mice were purchased from Charles River Laboratories (Kanagawa, Japan) and were housed in cages and provided nesting material, with food and water provided *ad libitum*, under light/dark conditions (lights on at 7:00 A.M., lights off at 9:00 P.M.) and temperature maintained at 23 °C – 26 °C.

2.2. Drugs

PTZ (Sigma-Aldrich Japan, Tokyo, Japan) was dissolved in saline at 20 mg/mL. (+)-MK-801 (dizocilpine hydrogen maleate; 130–17381, FUJIFILM Wako Pure Chemical Corporation, Osaka, Japan) was diluted in saline (0.1 mg/mL) and administered i.p. in a volume of 0.2 mg/kg. This dose was selected based on a previous study at 0.2 mg/kg in mice (Gray et al., 2009; Bygrave et al., 2016). α-pinene was acquired from FUJIFILM Wako Pure Chemical Corporation (169–21242). α-pinene was diluted in saline containing 5 % Tween-80 at a concentration of 20 mg/mL and administered i.p. in a volume of 20 mg/kg. This dose was selected based on previous studies (Yang et al., 2016).

2.3. Pentylenetetrazole-induced kindling procedure

All mice were randomized into four groups (n 15, per group). A dose of 40 mg/kg was injected i.p. once a day for a total period of 15 days. Vehicle control mice were injected with saline. Seizure events during a 30 min period, following each PTZ injection, were observed. The resultant seizures were scored as follows (Watanabe et al., 2011): Stage 0 (no response); stage 1 (ear and facial twitching); stage 2 (myoclonic body jerks); stage 3 (forelimb clonus, rearing); stage 4 (clonic convulsions, turn onto the side); stage 5 (generalized clonic convulsions, turn onto the back). To determine the effects of MK-801 and α-pinene on the PTZ-induced kindling progress, mice received either PTZ administration alone, or were pretreated with either MK-801, or α-pinene, 30 min prior to each PTZ injection. Treatments were administered once daily for a total of 15 injections. Duration of treatment was chosen based on our previous study and that of others (Li et al., 2014; Sun et al., 2019; Ueno et al., 2019a, 2019b). On the 16th day, mice were sacrificed, and their brains were removed.

2.4. Tissue preparation

Mice were anesthetized with a lethal dose of sodium pentobarbital (120 mg/kg, i.p.) and transcardially perfused with 25 mL of phosphate-buffered saline (PBS) followed by 100 mL of 4 % paraformaldehyde in PBS (pH 7.4). Brains were dissected and post-fixed overnight at 4 °C in the above fixative. The brains were then cryoprotected in 15 % sucrose for 12 h followed by 30 % sucrose for 20 h at 4 °C. Next, the brains were frozen in an optimum cutting temperature compound (Tissue-Tek; Sakura Finetek, Tokyo, Japan) using a slurry of normal hexane in dry ice. Serial coronal sections with a thickness of 40 μm were obtained at −20 °C using a cryostat (CM3050S; Leica Wetzlar, Germany). The sections were collected in ice-cold PBS containing 0.05 % sodium azide.

2.5. Immunohistochemistry

We treated the cryostat sections with 0.1 % Triton X-100 with PBS

at room temperature for 15 min. After three washes with PBS, we incubated the sections with 10 % normal goat serum (ImmunoBioScience Corp., Mukilteo, WA) in PBS at room temperature for 1 h. Sections were then washed three times with PBS, and incubated overnight at 4 °C in PBS containing biotinylated WFA (B-1355, Vector Laboratories; 1:200) and/or the antibodies described in the subsection "Antibodies and lectins." After washing with PBS, we incubated the sections with Alexa Fluor 594-conjugated streptavidin (S11227; Molecular Probes, Eugene, OR) and/or the corresponding secondary antibodies (described in the subsection "Antibodies and lectins") at room temperature for 2 h. We rinsed the labeled sections again with PBS and mounted them on glass slides with Vectashield medium (H-1400; Vector Laboratories, Funakoshi Co., Tokyo, Japan). We stored the prepared slides at 4 °C until microscopy analysis was performed.

2.6. Antibodies and lectins

We used the following lectins and primary antibodies for staining: biotinylated WFA (B-1355, Vector Laboratories; 1:200), mouse anti-parvalbumin (PV; clone PARV-19, P3088; Sigma-Aldrich Japan, Tokyo, Japan; 1:1000), mouse anti-NeuN (clone A60, MAB377; Millipore; 1:500), mouse anti-aggrecan (Cat-315; MAB1581, MERCK; 1:1000), rabbit anti-glial fibrillary acidic protein (GFAP; ab7260; Abcam, Cambridge, MA; 1:1000), rabbit anti-ionized calcium-binding adapter molecule 1 (Iba-1; 019–19741; FUJIFILM Wako Pure Chemical Corporation, Osaka, Japan; 1:1000), mouse anti-glutamic acid decarboxylase 67 (GAD67; clone 1 G10.2, MAB5406; Millipore, Bedford, MA; 1:1000), and guinea pig anti-vesicular glutamate transporter 1 (VGLUT1; AB5905; Millipore; 1:1000).

We used the following secondary antibodies for visualization: Alexa Fluor 488-conjugated goat anti-mouse IgG (ab150113; Abcam, Cambridge, MA; 1:1000), Alexa Fluor 594-conjugated goat anti-guinea pig (A-11076; Thermo Fisher Scientific, Waltham, MA; 1:500), FITC-conjugated anti-mouse IgM (sc-2082, Santa Cruz Biotechnology, Santa Cruz, CA, 1:1000), Texas Red-conjugated goat anti-rabbit (TI-1000; Vector Laboratories, Funakoshi Co., Tokyo, Japan), and streptavidin-conjugated Alexa Fluor 594 (S11227, Thermo Fisher Scientific; 1:1000).

2.7. Microscopy imaging

For quantification of the density of PV-, WFA-, and Cat-315-positive PNNs and analysis of ECM fluorescence intensities, we used confocal laser scanning microscopy (LSM700; Carl Zeiss, Oberkochen, Germany) to obtain images of stained sections. Images (1024 × 1024 pixels) were saved as TIFF files using ZEN software (Carl Zeiss). Briefly, we performed our analysis using a 10× objective lens and a pinhole setting that corresponded to a focal plane thickness of less than 1 μm. For observing ECM molecules, GAD67- and VGLUT1-positive synaptic terminals, samples were randomly selected and high-magnification images using a 100× objective lens were acquired. Prior to capture, the exposure time, gain, and offset were carefully set to ensure a strong signal, but to avoid saturation. Identical capture conditions were used for all sections. Images from whole sections were acquired using a 10× objective lens of a fluorescence microscope (BZ-X; KEYENCE, Tokyo, Japan) and we merged them using the KEYENCE BZ-X Analyzer software (KEYENCE).

2.8. Quantification of labeled PNNs and ECM

Brain regions were identified in accordance with the mouse brain atlas of Franklin and Paxinos (2012). From each mouse, four serial, coronal hippocampal sections were selected and processed for staining. All confocal images were acquired as TIFF files, and analyzed with the NIH ImageJ software (NIH, Bethesda, MD; http://rsb.info.nih.gov/nih-image/). Stained PNNs (soma size above 60 μm^2) were manually tagged and counted within the area of interest. Background intensities were subtracted using unstained portions (region of the nucleolus) of each section. Labeled neuron density was calculated as cells/mm^2. Quantifications were performed by a blinded, independent observer. For quantifying the fluorescence intensity of ECM-positive molecules, GAD67- and VGLUT1-positive synaptic terminals, WFA-, and Cat-315-positive PNNs, we selected four sections from each mouse brain and stained as described above. The ellipses circumscribing the WFA-, and Cat-315-positive PNNs were traced manually on 8-bit images of each section, and the gray levels for WFA or Cat-315 labeling were measured using the ImageJ software, which was assigned arbitrary units (a.u.). We manually outlined the parts excluding PNNs and measured the gray level with NIH ImageJ. Background intensities were subtracted using unstained portions of each section. We acquired all confocal images as TIFF files and analyzed them with NIH ImageJ. We coded the slides and a blinded, independent observer quantified them.

2.9. Data analysis

Data are expressed as box plots of five animals per group. Statistical significance, set at $p < 0.05$, was determined by two-way analysis of variance followed by Bonferroni t-tests.

3. Results

3.1. Effect of MK-801 and α-pinene in the pentylenetetrazole-induced kindling mouse model

Repeated administration of PTZ (40 mg/kg) over a period of 15 days resulted in a steady increase in seizure scores, effectively inducing kindling in mice (Fig. 1A). Administration of MK-801 prior to each PTZ injection, decreased seizure severity. In addition, pretreatment with α-pinene, prior to each PTZ injection, was found to suppress the increase in seizure score in comparison with the PTZ only group (Fig. 1A). Pretreatment with MK-801, or α-pinene, also significantly changed the maximal seizure score distribution on the 15th day (Fig. 1B). Furthermore, the lethality rate following the PTZ injections, decreased significantly in response to pretreatment with α-pinene (Fig. 1C). 0 % lethality rate was observed in PTZ-kindled, MK-801-treated mice (Fig. 1C).

3.2. Effect of MK-801 and α-pinene on PV-positive neurons, WFA-positive and Cat-315-positive PNNs in the PTZ-kindled mouse hippocampus

PV-positive mouse hippocampal neurons were observed and compared among experimental groups (Fig. 2**A-D** and 3 A). To examine the spatial distribution of PNNs and ECM molecules, we stained for WFA (Fig. 2**E-H,** 3 **A**), and Cat-315 (Fig. 2**I-L,** 3 **A**). The distribution of PV-positive neurons, and WFA-positive/Cat-315-positive PNNs in the hippocampus was very similar in all groups.

We quantified PV-positive neurons, and WFA-positive and Cat-315-positive PNNs in the hippocampi of different treatment groups (Fig. 3**B-D,** Table 1**A-C**). In the CA1 hippocampal region, the density of PV-positive neurons was significantly lower in α-pinene treated, PTZ-induced mice than in control mice (Fig. 3B, Table 1**A**). In the CA3 region, both MK-801 and α-pinene pretreatments, significantly attenuated the increased density of PV-positive neurons induced by PTZ administration (Fig. 3B, Table 1**A**). In the CA1 region, the density of WFA-positive PNNs was significantly lower in MK-801 treated, PTZ-induced mice than in PTZ-kindled mice (Fig. 3C, Table 1**B**). In the CA3 region, both MK-801 and α-pinene pretreatments, significantly attenuated the increased density of WFA-positive PNNs induced by PTZ administration (Fig. 3C, Table 1**B**). In the CA3 region, the density of Cat-315-positive PNNs, in both MK-801 treated, PTZ-induced and α-pinene treated, PTZ-induced mice, was significantly lower than in PTZ-kindled mice (Fig. 3D, Table 1**C**). In other regions, there was no significant difference in the density of Cat-315-positive PNNs between the four groups

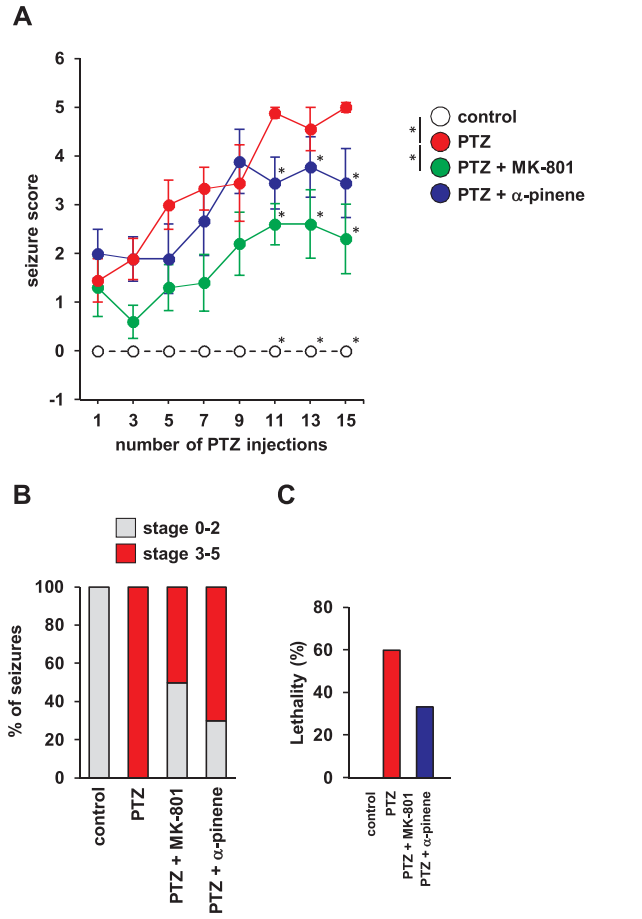

Fig. 1. Effect of MK-801 and a-pinene on PTZ-induced kindling.
(A) Graphs showing the seizure score as assessed on the 1st, 3rd, 5th, 7th, 9th, 11th, 13th, and 15th day of the study. Data are expressed as the mean ± SEM. *p < 0.05 versus saline-treated mice. The p-values were calculated using the repeated measures ANOVA in A. (B) Distribution of mice by maximal seizure score on the 15th day of the study. (C) Percent lethality in different treated groups.

(Fig. 3D, Table 1**C**).

To examine whether PNNs are associated with PV-positive neurons in the mouse hippocampi of different experimental groups, we conducted a quantitative analysis (Fig. 3**E-H,** Table 1**D-G**). In the CA1 region, the percentage of PV-positive neurons, not surrounded by both WFA-positive and Cat-315-positive PNNs, in the PTZ-kindled mice was significantly lower than in both control mice and α-pinene treated, PTZ-induced mice (Fig. 3E, Table 1**D**). In the CA3 area, the percentage of PV-positive neurons, not surrounded by both WFA-positive and Cat-315-positive PNNs, in the PTZ-kindled mice, was significantly lower than in control mice (Fig. 3E, Table 1**D**). In the dentate gyrus (DG) area, the percentage of PV-positive neurons, surrounded by both WFA- and Cat-315-positive PNNs, in MK-801 treated, PTZ-induced mice was significantly lower than in α-pinene treated, PTZ-induced mice (Fig. 3F, Table 1**E**). In the CA1 region, the percentage of PV-positive neurons, surrounded by WFA-positive PNNs in the PTZ-kindled mice, was significantly higher than in both control mice and α-pinene treated, PTZ-induced mice (Fig. 3G, Table 1**F**). In the DG area, the percentage of PV-positive neurons, surrounded by WFA-positive PNNs, in α-pinene treated, PTZ-induced mice, was significantly higher than in MK-801 treated, PTZ-induced mice (Fig. 3G, Table 1**F**). There were no significant differences in the percentage of PV-positive neurons, surrounded by Cat-315-positive PNNs, between the four experimental groups in most of the areas that we examined (Fig. 3H, Table 1**G**).

3.3. Effect of MK-801 and α-pinene on PV-positive, WFA-positive, and Cat-315-positive fluorescence intensity in the PTZ-kindled mouse hippocampus

To analyze the effect of PTZ-kindling on the expression of PV protein, we analyzed the fluorescence intensity of PV-positive neurons in the hippocampi of different experimental groups (Fig. 4A, Table 1**H**). In both the CA1 and CA3 areas of the hippocampus, both MK-801 and α-pinene pretreatments significantly attenuated the increased PV fluorescence intensity induced by PTZ administration (Fig. 4A, Table 1**H**). In the DG area, PV fluorescence intensity was lower in MK-801 treated, PTZ-induced mice than in the other three groups (Fig. 4A, Table 1**H**).

To analyze the effect of MK-801 and α-pinene on the expression of WFA-positive, and Cat-315-positive molecules in the PTZ-kindled mouse hippocampus, we analyzed the fluorescence intensity of each WFA-positive PNN, and Cat-315-positive PNN, in different treatment groups (Fig. 4B**, C,** Table 1**I, J**). In the CA1 area, WFA fluorescence intensity was lower in α-pinene treated, PTZ-induced mice than in the other three groups (Fig. 4B, Table 1**I**). In the CA3 area, MK-801 pretreatment significantly attenuated the increased WFA fluorescence intensity induced by PTZ administration (Fig. 4B, Table 1**I**). In the CA1 area, Cat-315 fluorescence intensity was lower in α-pinene treated, PTZ-induced mice than in both PTZ-kindled mice and MK-801 treated, PTZ-induced mice (Fig. 4C, Table 1J). In the CA3 area, Cat-315 fluorescence intensity was lower in MK-801 treated, PTZ-induced mice than in PTZ-kindled mice (Fig. 4C, Table 1J). In the DG area, Cat-315 fluorescence intensity was lower in MK-801 treated, PTZ-induced mice than in control mice (Fig. 4C, Table 1J).

Next, we analyzed WFA-positive and Cat-315-positive molecules, excluding PNNs, in each experimental group (Fig. 4D**, E,** Table 1**K, L**). In the CA1 area, the mean fluorescence intensity of WFA-positive molecules, excluding PNNs, was lower in α-pinene treated, PTZ-induced mice than in the other three groups (Fig. 4D, Table 1**K**). In the CA3 area, the mean fluorescence intensity of WFA-positive molecules, excluding PNNs, was lower in control mice than in the other three groups (Fig. 4D, Table 1**K**). In the CA1 area, the mean fluorescence intensity of Cat-315-positive molecules, excluding PNNs, in both MK-801 treated, PTZ-induced and α-pinene treated, PTZ-induced mice was significantly lower than in PTZ-kindled mice (Fig. 4E, Table 1**L**). In the CA3 area, the mean fluorescence intensity of Cat-315-positive molecules, excluding PNNs, in both MK-801 treated, PTZ-induced and α-pinene treated, PTZ-induced mice were significantly lower than in PTZ-kindled mice (Fig. 4E, Table 1**L**).

3.4. Effect of MK-801 and α-pinene on GFAP-positive astrocytes and Iba-1-positive microglia in the PTZ-kindled mouse hippocampus

To analyze the effects of MK-801 and α-pinene on astrocytosis induced by PTZ-kindling, we analyzed GFAP-positive astrocytes in the CA1 hippocampal region of different treatment groups (Fig. 5**A-D**). GFAP-positive astrocytes appeared ramified, forming more spreading branches in the CA1 of PTZ-kindled, MK-801 treated, PTZ-induced, and α-pinene treated, PTZ-induced mice compared with controls. We quantified the GFAP-positive areas of the CA1 in different treatment groups (Fig. 5I, Table 1**M**). In the SO area of the CA1 region, we found that the GFAP-positive area in MK-801 treated, PTZ-induced mice was lower than in the PTZ-kindled mice. In the SR area of the CA1 region, the GFAP-positive areas in both MK-801 treated, PTZ-induced and α-pinene treated, PTZ-induced mice were significantly lower than in PTZ-kindled mice.

To examine the effects of MK-801 and α-pinene on immune activation induced by PTZ-kindling, the morphology of Iba-1-positive microglia in the CA1 was examined (Fig. 5**E-H**). In the CA1 area, there was no significant difference in the morphology of Iba-1-positive microglia between our four experimental groups.

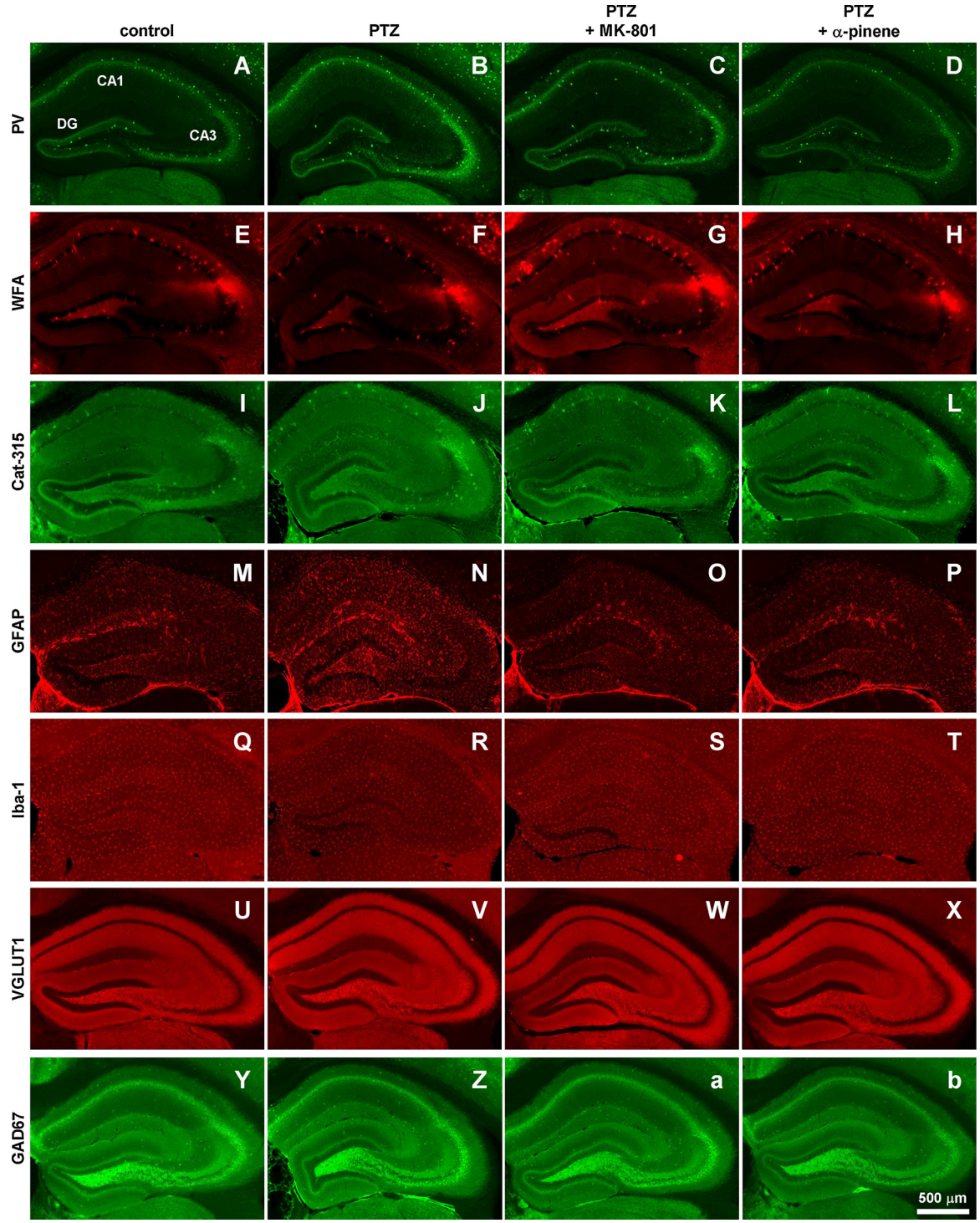

Fig. 2. PV, WFA, Cat-315, GFAP, Iba-1, VGLUT1, and GAD67-positive images in different treated group mouse hippocampus.
Representative images of PV-positive neurons (A–D), WFA-positive molecules (E–H), Cat-315-positive molecules (I–L), GFAP-positive cells (M–P), Iba-1-positive microglia (Q–T), VGLUT1-positive puncta (U–X), and GAD67-positive puncta (Y-b) in the mouse hippocampus of control (A, E, I, M, Q, U, Y), PTZ-kindled (B, F, J, N, R, V, Z), PTZ-kindled MK-801-treated (C, G, K, O, S, W, a), and PTZ-kindled a-pinene treated mice (D, H, L, P, T, X, b). Scale bars: 500 μm in b (applies to A–Z, a–b).

3.5. Effects of MK-801 and α-pinene on glutamatergic and GABAergic synaptic terminals in the PTZ-kindled mouse hippocampus

To examine the effects of MK-801 and α-pinene on the alteration of synaptic terminals induced by PTZ-kindling, we labeled both VGLUT1-positive synaptic terminals and GAD67-positive synaptic terminals (Fig. 6**A-H**). VGLUT1- and GAD67-positive synaptic terminals were expressed in the neuropil of the mouse hippocampi (Fig. 6**A-H**). We quantified area-specific VGLUT1- and GAD67-positive signal intensities, excluding GAD67-positive neurons, in the CA1 areas (Fig. 6I, J, Table 1N, O).

In the SO area of the CA1 region, VGLUT1 fluorescence intensity in MK-801 treated, PTZ-induced mice was significantly lower than in both PTZ-kindled and α-pinene treated PTZ-induced mice (Fig. 6I, Table 1**N**). In the SR area of the CA1 region, VGLUT1 fluorescence intensity in α-pinene treated, PTZ-induced mice was significantly higher

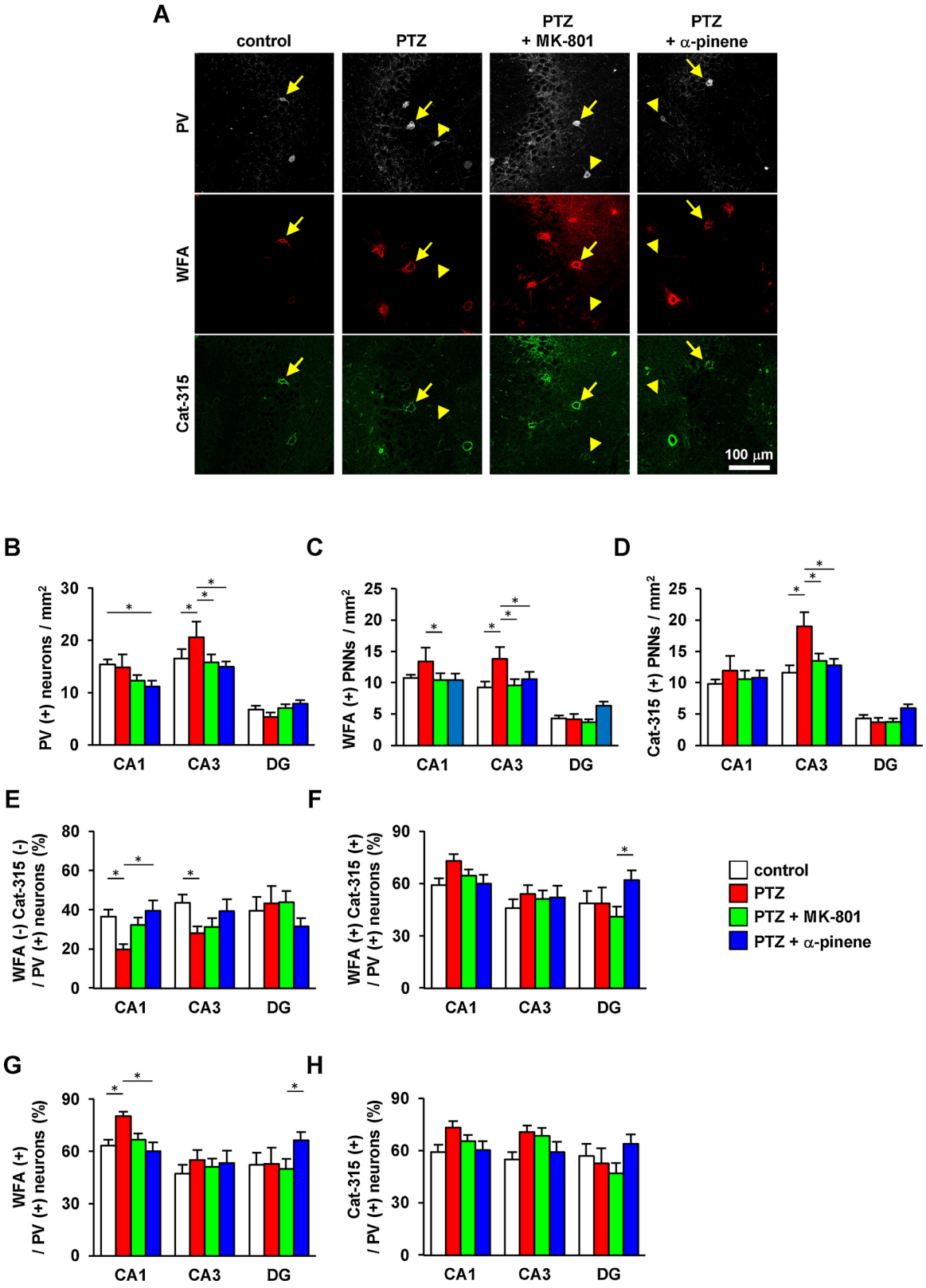

Fig. 3. The densities of PV-positive neurons, WFA-positive, and Cat-315-positive PNNs in different treated group mouse hippocampus.
Representative triple immunofluorescent images of PV-positive neurons, WFA-positive PNNs, and Cat-315-positive PNNs in the CA3 of control, PTZ-kindled, PTZ-kindled MK-801-treated, and PTZ-kindled α-pinene treated mice (A). The arrows indicate PV-positive neurons co-localized with PNN markers. The arrowheads indicate PV-positive neurons not co-localized with PNN markers. Region-specific patterns of PV-positive neuron density (B), WFA-positive PNN density (C), and Cat-315-positive PNN density (D) are shown. The percentage of PV-positive neurons that do not contain both WFA- and Cat-315-positive PNNs (E), the percentage of PV-positive neurons that contain both WFA- and Cat-315-positive PNNs (F), the percentage of PV-positive neurons that contain WFA-positive PNNs (G), and the percentage of PV-positive neurons that contain Cat-315-positive PNNs (H) in the hippocampus are shown. Data are presented as the mean ± SEM (n = 6 mice per group). The p values indicate two-way ANOVA by Bonferroni t-test. *$p < 0.05$ for comparison between different treated groups in the same region. Respective p values are listed in Table 1. Scale bars: 100 μm in A.

Table 1
P values for Figs. 3–6.

				A. Fig. 3B PV neurons	B. Fig. 3C WFA-positive PNNs	C. Fig. 3D Cat-315-positive PNNs
CA1	control	vs	PTZ	0.778	0.105	0.249
	control	vs	PTZ + MK801	0.073	0.67	0.703
	control	vs	PTZ + α-pinene	0.022	0.882	0.306
	PTZ	vs	PTZ + MK801	0.225	0.043	0.385
	PTZ	vs	PTZ + α-pinene	0.101	0.076	0.752
	PTZ + MK801	vs	PTZ + α-pinene	0.585	0.775	0.498
CA3	control	vs	PTZ	0.042	0.004	< 0.001
	control	vs	PTZ + MK801	0.591	0.875	0.297
	control	vs	PTZ + α-pinene	0.279	0.4368	0.679
	PTZ	vs	PTZ + MK801	0.013	0.004	< 0.001
	PTZ	vs	PTZ + α-pinene	0.003	0.022	< 0.001
	PTZ + MK801	vs	PTZ + α-pinene	0.564	0.515	0.519
DG	control	vs	PTZ	0.706	0.626	0.771
	control	vs	PTZ + MK801	0.947	0.722	0.84
	control	vs	PTZ + α-pinene	0.602	0.202	0.416
	PTZ	vs	PTZ + MK801	0.655	0.418	0.634
	PTZ	vs	PTZ + α-pinene	0.402	0.538	0.68
	PTZ + MK801	vs	PTZ + α-pinene	0.634	0.09	0.29

				D. Fig. 3E WFA^- $Cat\text{-}315^-$ PNNs / PV neurons	E. Fig. 3F WFA^+ $Cat\text{-}315^+$ PNNs / PV neurons	F. Fig. 3G WFA^+ PNNs / PV neurons	G. Fig. 3H $Cat\text{-}315^+$ PNNs / PV neurons
CA1	control	vs	PTZ	0.03	0.446	0.047	0.438
	control	vs	PTZ + MK801	0.531	0.463	0.624	0.349
	control	vs	PTZ + α-pinene	0.658	0.899	0.675	0.927
	PTZ	vs	PTZ + MK801	0.087	0.865	0.121	0.988
	PTZ	vs	PTZ + α-pinene	0.01	0.502	0.022	0.474
	PTZ + MK801	vs	PTZ + α-pinene	0.268	0.532	0.346	0.384
CA3	control	vs	PTZ	0.04	0.385	0.349	0.078
	control	vs	PTZ + MK801	0.073	0.482	0.576	0.132
	control	vs	PTZ + α-pinene	0.53	0.412	0.388	0.351
	PTZ	vs	PTZ + MK801	0.573	0.774	0.63	0.609
	PTZ	vs	PTZ + α-pinene	0.12	0.862	0.836	0.321
	PTZ + MK801	vs	PTZ + α-pinene	0.232	0.894	0.745	0.56
DG	control	vs	PTZ	0.841	0.844	0.955	0.279
	control	vs	PTZ + MK801	0.521	0.305	0.739	0.209
	control	vs	PTZ + α-pinene	0.247	0.08	0.054	0.389
	PTZ	vs	PTZ + MK801	0.725	0.274	0.737	0.95
	PTZ	vs	PTZ + α-pinene	0.225	0.185	0.117	0.068
	PTZ + MK801	vs	PTZ + α-pinene	0.062	0.004	0.019	0.029

				H. Fig. 4A PV fluorescence	I. Fig. 4B WFA fluorescence	J. Fig. 4C Cat-315 fluorescence
CA1	control	vs	PTZ	< 0.001	0.261	0.014
	control	vs	PTZ + MK801	0.081	0.5	0.168
	control	vs	PTZ + α-pinene	< 0.001	0.001	0.441
	PTZ	vs	PTZ + MK801	< 0.001	0.591	0.202
	PTZ	vs	PTZ + α-pinene	< 0.001	< 0.001	0.002
	PTZ + MK801	vs	PTZ + α-pinene	0.034	< 0.001	0.035
CA3	control	vs	PTZ	< 0.001	< 0.001	< 0.001
	control	vs	PTZ + MK801	0.031	0.349	0.316
	control	vs	PTZ + α-pinene	0.342	0.041	0.025
	PTZ	vs	PTZ + MK801	< 0.001	0.005	0.004
	PTZ	vs	PTZ + α-pinene	< 0.001	0.064	0.098
	PTZ + MK801	vs	PTZ + α-pinene	0.001	0.281	0.203
DG	control	vs	PTZ	0.566	0.712	0.264
	control	vs	PTZ + MK801	< 0.001	0.887	0.001
	control	vs	PTZ + α-pinene	0.821	0.372	0.125
	PTZ	vs	PTZ + MK801	< 0.001	0.78	0.22
	PTZ	vs	PTZ + α-pinene	0.684	0.739	0.959
	PTZ + MK801	vs	PTZ + α-pinene	< 0.001	0.387	0.128

				K. Fig. 4D WFA fluorescence	L. Fig. 4E Cat-315 fluorescence
CA1: so	control	vs	PTZ	0.193	< 0.001
	control	vs	PTZ + MK801	0.567	< 0.001
	control	vs	PTZ + α-pinene	< 0.001	< 0.001
	PTZ	vs	PTZ + MK801	0.404	< 0.001
	PTZ	vs	PTZ + α-pinene	0.003	< 0.001
	PTZ + MK801	vs	PTZ + α-pinene	< 0.001	0.339
CA1: sr	control	vs	PTZ	0.844	< 0.001

(*continued on next page*)

Table 1 (*continued*)

				K. Fig. 4D WFA fluorescence	L. Fig. 4E Cat-315 fluorescence
	control	vs	PTZ + MK801	0.58	< 0.001
	control	vs	PTZ + α-pinene	0.107	< 0.001
	PTZ	vs	PTZ + MK801	0.495	< 0.001
	PTZ	vs	PTZ + α-pinene	0.109	< 0.001
	PTZ + MK801	vs	PTZ + α-pinene	0.276	0.536
CA3: so	control	vs	PTZ	< 0.001	< 0.001
	control	vs	PTZ + MK801	< 0.001	0.089
	control	vs	PTZ + α-pinene	< 0.001	0.829
	PTZ	vs	PTZ + MK801	0.167	< 0.001
	PTZ	vs	PTZ + α-pinene	0.155	< 0.001
	PTZ + MK801	vs	PTZ + α-pinene	0.946	0.048
CA3: sr	control	vs	PTZ	0.021	< 0.001
	control	vs	PTZ + MK801	0.005	< 0.001
	control	vs	PTZ + α-pinene	< 0.001	0.05
	PTZ	vs	PTZ + MK801	0.955	< 0.001
	PTZ	vs	PTZ + α-pinene	0.539	< 0.001
	PTZ + MK801	vs	PTZ + α-pinene	0.503	0.074

				M. Fig. 5I % GFAP$^+$ area	N. Fig. 6I VGLUT1 fluorescence	O. Fig. 6J GAD67 fluorescence
CA1: so	control	vs	PTZ	< 0.001	< 0.001	0.003
	control	vs	PTZ + MK801	0.006	0.007	0.949
	control	vs	PTZ + α-pinene	< 0.001	< 0.001	< 0.001
	PTZ	vs	PTZ + MK801	0.023	< 0.001	0.002
	PTZ	vs	PTZ + α-pinene	0.145	0.673	< 0.001
	PTZ + MK801	vs	PTZ + α-pinene	0.404	< 0.001	< 0.001
CA1: sr	control	vs	PTZ	< 0.001	< 0.001	0.001
	control	vs	PTZ + MK801	< 0.001	< 0.001	< 0.001
	control	vs	PTZ + α-pinene	< 0.001	< 0.001	< 0.001
	PTZ	vs	PTZ + MK801	0.004	0.793	< 0.001
	PTZ	vs	PTZ + α-pinene	0.052	0.011	< 0.001
	PTZ + MK801	vs	PTZ + α-pinene	0.333	0.005	< 0.001

*Significant difference compared with control mice in the same region ($p < 0.05$).

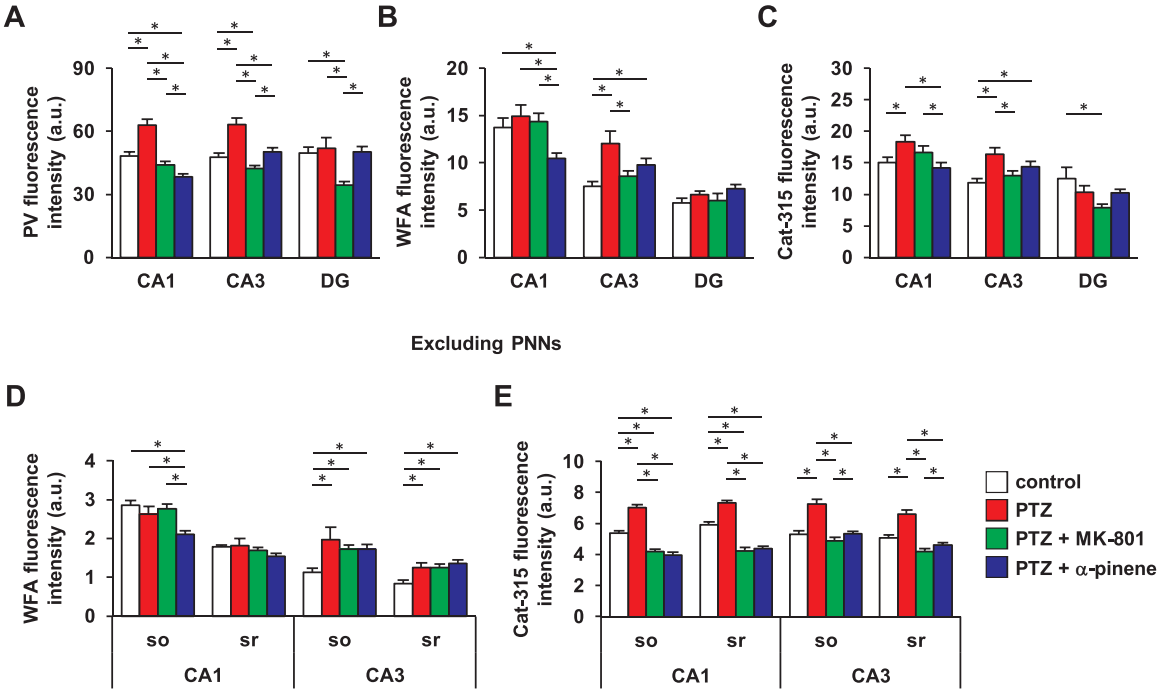

Fig. 4. Quantitative analyses of extracellular matrix molecules in the different treated group mouse hippocampus.
Quantified mean fluorescence intensity of PV-positive neurons (A), WFA-positive PNNs (B), Cat-315-positive PNNs (C), in the mouse hippocampus. Quantified mean fluorescence intensity of WFA-positive molecules (D), and Cat-315-positive molecules (E), excluding the PNN, in the mouse hippocampus. Data are presented as the mean ± SEM (n = 6 mice per group). The p values indicate two-way ANOVA by Bonferroni t-test. *$p < 0.05$ for comparison between different treated groups in the same region. Respective p values are listed in Table 1.

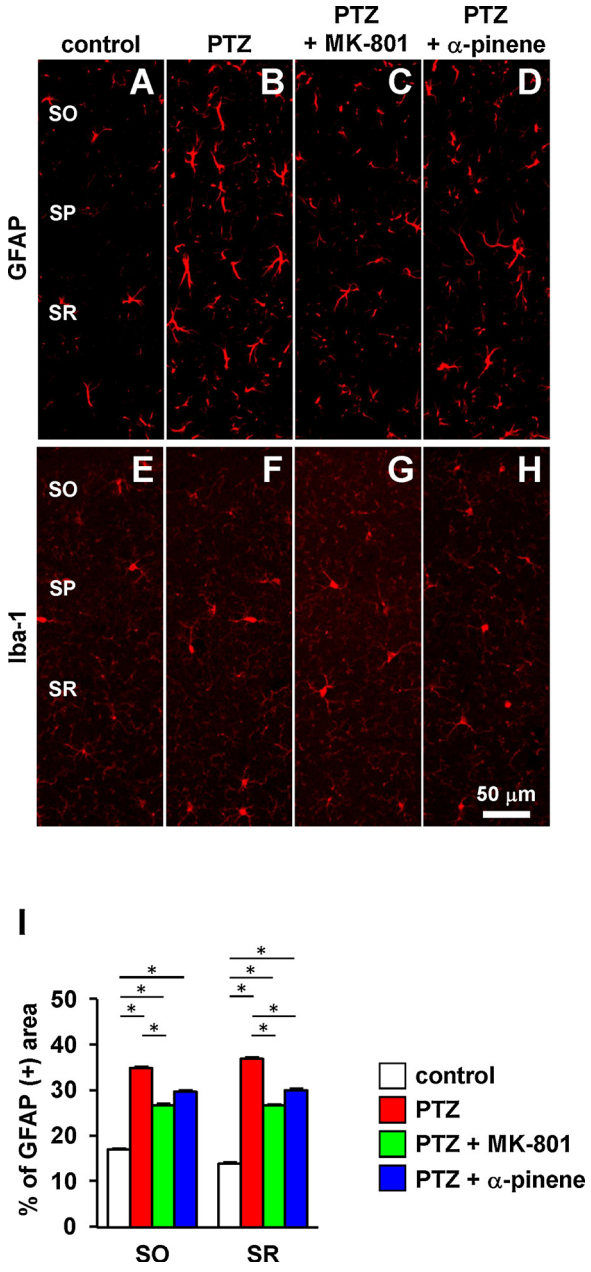

Fig. 5. Immunohistochemical analysis of the GFAP-positive astrocytes in the different treated group mouse hippocampus.
Representative immunofluorescent images of GFAP-positive astrocytes (A–D) and Iba-1-positive microglia (E–H) in the CA1 of control (A, E), PTZ-kindled (B, F), PTZ-kindled MK-801-treated (C, G), and PTZ-kindled a-pinene treated mice (D, H). Quantified the percentage of GFAP-positive area in the SO and SR of the CA1 of the different treated group mouse (I). Data are presented as the mean ± SEM (n = 6 mice per group). The p values indicate two-way ANOVA by Bonferroni t-test. *$p < 0.05$ for comparison between different treated groups in the same region. Scale bars: 50 μm in H (applies to A–H). Respective p values are listed in Table 1.

than in both PTZ-kindled and MK-801 treated, PTZ-induced mice.

In both the SO and SR areas of the CA1 region, GAD67 fluorescence intensity in both MK-801 treated, PTZ-induced and α-pinene treated, PTZ-induced mice was significantly lower than in PTZ-kindled mice (Fig. 6J, Table 1**O**).

4. Discussion

In this study, we showed that MK-801 and α-pinene inhibit PTZ-induced kindling acquisition. Furthermore, our results show that MK-801 and α-pinene influence the activation of astrocytes as well as the increase of ECM expression induced by PTZ. This result provides a new insight into epilepsy development and may influence the development of new therapeutic agents for epilepsy treatment.

In the PTZ provocation test, prior administration of MK-801 significantly suppressed status epilepticus and exerted an antiepileptic effect. Repeated administration of PTZ-induced severe seizures and high mortality (Ammon-Treiber et al., 2007; Hussein et al., 2019). MK-801 effectively reduced seizure severity and reduced mortality in PTZ kindling mice. Several studies have shown that NMDA receptor antagonists delay kindling acquisition and prevent the onset of seizures (Dingledine et al., 1990).

In this study, α-pinene suppressed kindling acquisition by preventing an increase in seizures by PTZ. However, during the first few administrations of PTZ, α-pinene pre-administration did not appear to attenuate seizures. In fact, it has been shown that α-pinene differs from β-pinene in action and has no anticonvulsant action (Felipe et al., 2019). Although the results of this study are consistent with previous studies, we report the novel kindling inhibitory effect of α-pinene. As with MK-801, increasing the dose of α-pinene may eliminate mortality. Further studies are warranted to verify the action of α-pinene.

In the present study, the kindling model showed activation of astrocytes but not microglia. In PTZ provocation tests, prior administration of MK-801 significantly suppressed astrocyte activation in the hippocampus. Reactive astrocytes are observed in the hippocampus of epilepsy animal models (Borges et al., 2003; Shapiro et al., 2008), and in the human hippocampus with temporal lobe epilepsy (Cohen-Gadol et al., 2004). PTZ administration increases glutamate secretion in the brain (Cremer et al., 2009). Glutamate induces astrocyte activation (as measured by morphological changes and GFAP expression) in neuronal / astrocyte co-cultures, or cultured astrocytes (Edling et al., 2007; Montes de Oca Balderas and Montes de Oca Balderas, 2018). However, this effect is blocked by MK-801 or ifenprodil, but only in neuron / astrocyte co-cultures. We have shown that MK-801 administration suppresses PTZ-induced astrocyte activation, to the best of our knowledge, for the first time. Astrocytes express the NMDA receptor (Skowrońska et al., 2019). Dose-dependent astrocytes are affected by the NMDA receptor-specific antagonist, MK-801 (Zhou et al., 2010). The detailed mechanism by which MK-801 suppresses astrocyte activation remains to be elucidated. However, the well-known NMDA receptor channel blocker, memantine, has been reported to exert anticonvulsant effects during maximal electric shock attacks (Parsons et al., 1995; Urbańska et al., 1992). There is evidence that another NMDA receptor channel blocker, ketamine, is useful for treating refractory status epilepticus (Dorandeu et al., 2013). MK-801 is suspected to have the same mechanism as these drugs, but further studies are warranted to investigate the mechanism by which PTZ-induced activation of astrocytes is suppressed. Although MK-801 acts as an anticonvulsant, it can cause Olney's lesions and induce cognitive impairment in experimental rats (Coan et al., 1987; Murray et al., 1995, 1997). Therefore, even if the antiepileptic effect of MK-801 is established, it cannot be used clinically. This study suggests that chemicals with a similar mechanism of action as MK-801 have new therapeutic potential against epilepsy.

In PTZ provocation tests, prior administration of α-pinene significantly suppressed astrocyte activation in the hippocampus. Previous studies have shown that α-pinene protects astrocytes from hydrogen peroxide-induced oxidative stress cellular damage (Porres-Martínez et al., 2015). Furthermore, monoterpenes such as α-pinene, citronellal, citronellol, and myrcene antagonize NMDA receptors (Guimarães et al., 2013). The detailed mechanism of α-pinene acting on astrocytes remains unknown, but it is possible that it may affect the astrocyte NMDA receptor. Further studies are warranted to elucidate the underlying mechanism.

PTZ administration increased the PV neuron density in the CA3

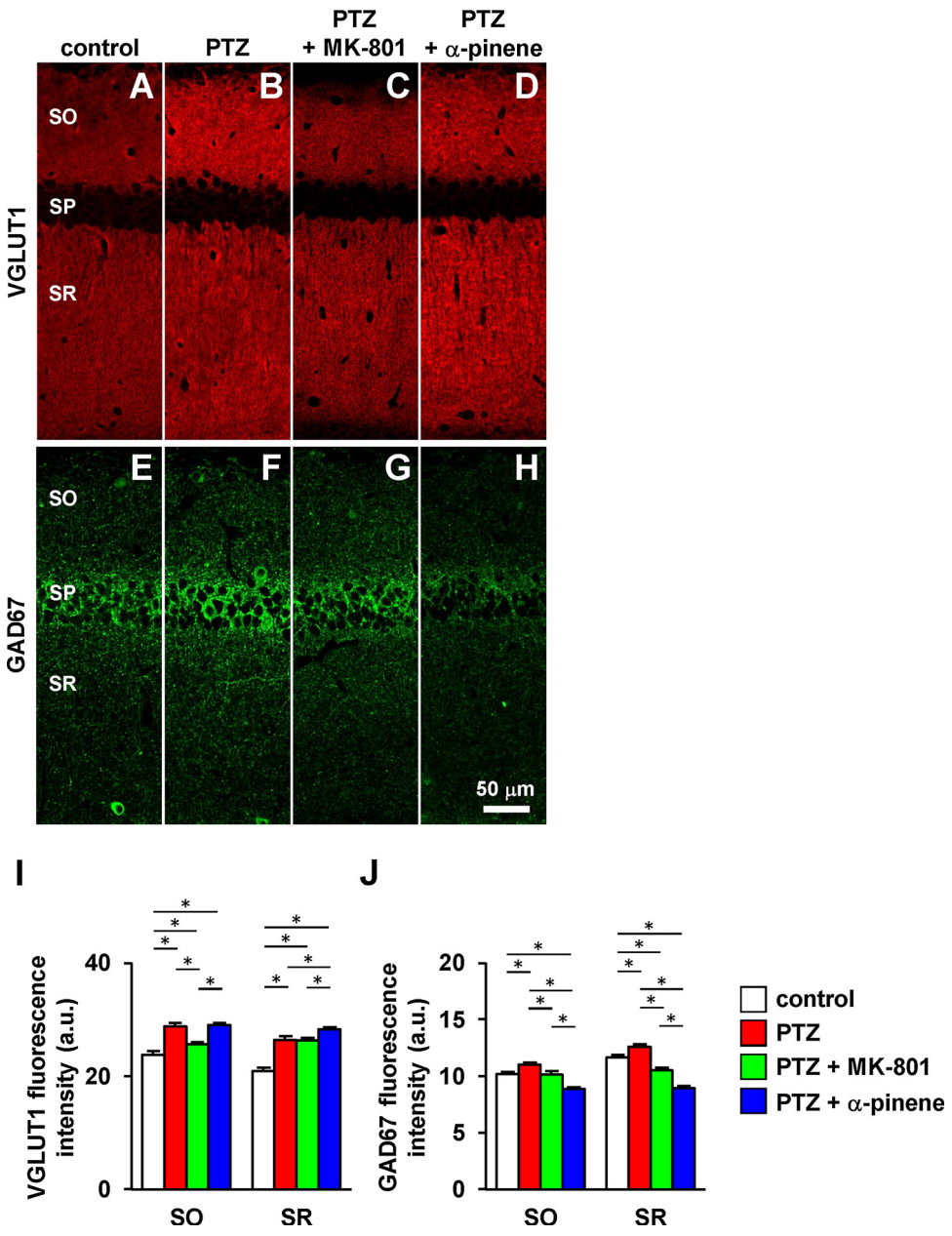

Fig. 6. Distribution of VGLUT1-positive and GAD67-positive puncta in the different treated group mouse hippocampus.
Representative immunofluorescent images of VGLUT1-positive puncta (A–D) and GAD67-1-positive puncta (E–H) in the CA1 of control (A, E), PTZ-kindled (B, F), PTZ-kindled MK-801-treated (C, G), and PTZ-kindled a-pinene treated mice (D, H). Quantified mean fluorescence intensity of VGLUT1-positive puncta (I) and GAD67-positive puncta (J), excluding the GAD67-positive neurons, in the SO and SR of the CA1 of the different treated group mouse. Data are presented as the mean ± SEM (n = 6 mice per group). The p values indicate two-way ANOVA by Bonferroni t-test. *$p < 0.05$ for comparison between different treated groups in the same region. Scale bars: 50 μm in H (applies to A–H). Respective p values are listed in Table 1.

region. It remains unclear whether the number of PV-positive neurons increased or if the GABAergic interneurons increased PV expression. In the PV-positive neurons of the sensory cortex, the expression level of PV proteins depends on sensory input (Caballero et al., 2013). The increase of PV neuron density in the CA3 region, therefore, may be correlated with the increase of PV protein expression.

In this study, MK-801 was shown to suppress the increase of WFA- and Cat-315-positive PNNs, and other ECM molecules induced by PTZ. We have previously shown that WFA- and Cat-315-positive PNNs increased in the hippocampus after kindling acquisition (Ueno et al., 2019a, 2019b), while other studies have shown that PNNs are formed in a stimulus-dependent manner (Lensjø et al., 2017; Ueno et al., 2017a, 2017b). The increased formation of PNNs preserves the repetitively stimulated pathways during PTZ administration. In fact, patients with temporal lobe epilepsy have elevated levels of chondroitin sulfate proteoglycan (CSPG), the main component of brain ECM (Perosa et al., 2002; Peixoto-Santos et al., 2017). The extracellular space is recognized as an important mediator of neuronal plasticity (Berardi et al., 2004). During regeneration following a spinal cord injury, ECM molecules suppress axonal extension (Gaudet and Popovich, 2014). Therefore, the increase in expression of ECM molecules in extracellular spaces observed in PTZ-kindling mice suggests a decrease in the hippocampal synaptic plasticity.

Loss of ECM components and degradation and removal of the ECM have been shown to inhibit kindling acquisition in an epilepsy mouse model (Hoffmann et al., 2009; Bausch, 2006). Therefore, blocking the increase in the numbers of ECM molecules may have an antiepileptic effect. Drugs that target ECM synthesis and degradation have been proven to be effective antiepileptic treatments (Dityatev, 2010).

In addition, astrocytes produce ECM molecules such as CSPG, and aggrecan (Wiese et al., 2012; Johnson et al., 2015), and the administration of MK-801 can block astrocyte activation and attenuate ECM production. In this study, MK-801 administration attenuated the PTZ-induced activation of astrocytes and ECM increase. However, blocking astrocyte activation may not be a direct consequence of blocking ECM. Indeed, it has been suggested that suppression of astrocyte activation by MK-801 may lead to suppression of epileptogenesis. The primary components of PNN are ECM hyaluronic acid, tenascin, and members of

the lectican family of chondroitin sulfate proteoglycans, such as aggrecan, versican, brevican, and neurocan (Bandtlow and Zimmermann, 2000; Yamaguchi, 2000). Further research is warranted to investigate ECM changes.

In this study, we show that the administration of α-pinene suppressed the increase of WFA- and Cat-315-positive PNNs, and ECM molecules just as well as MK-801 administration. In the CA3 region, α-pinene suppressed the increase of PNN density by PTZ administration, but did not completely suppress the increase of WFA-positive fluorescence intensity and Cat-315-positive fluorescence intensity. This suggests that α-pinene suppressed PNN formation around new PV-positive neurons but could not suppress the increased expression of ECM molecules in PNN. Although the detailed mechanism of the PTZ-induced astrocyte activation and the attenuation of the PTZ-induced ECM increase by α-pinene is unknown, the present study shows that the administration of α-pinene may be effective in blocking the ECM increase by PTZ.

Administration of MK-801 significantly reduced the increase in expression of PV protein by PTZ. The expression level of PV protein depends on the input stimulus (Caballero et al., 2013). Furthermore, PNN-covered neurons, have higher PV protein expression than PV neurons not covered with PNNs (Yamada et al., 2015; Ueno et al., 2017a, 2017b). In this study, PTZ kindling acquisition led to an increase in the number of PNNs. PTZ induces a state of increased neural excitation in the hippocampus (Squires et al., 1984). Also, in the hippocampus, the expression of PV protein may be increased by high excitability due to status epilepticus. In the groups in which MK-801, or α-pinene were administered, the increase in PNN formation by PTZ was attenuated. This suggests that MK-801 and α-pinene reduced the PTZ-induced PV protein expression.

However, MK-801 and α-pinene treatments were unable to completely block the increase of VGLUT1 by PTZ. MK-801 reduced the increase of VGLUT1 in the SO area of the CA1, but had no effect in the SR area of the CA1. In animal models of epilepsy, an increase of VGLUT1 in the hippocampus has been shown (Tannenberg and Dodd, 2009). An increase in GAD67 was confirmed by the acquisition of PTZ kindling which may suppress excessive neuronal excitation (Souchet et al., 2015). A disturbance in the balance of inhibitory and excitatory neurotransmitters is associated with epileptogenesis (Svenningsen et al., 2006).

Currently, numerous antiepileptic drugs are available worldwide for the treatment of epilepsy. Recent clinical and experimental evidence suggests the association between epilepsy activity and microglial and astrocyte activation and proliferation (Cohen-Gadol et al., 2004; de Lanerolle et al., 2010). The present study shows that new therapeutic agents targeting the inhibition of astrocyte activation and extracellular matrix increase may be useful as antiepileptic drugs.

The results of this study show, albeit indirectly, an increase in neural excitation in the hippocampus; however, MK-801 and α-pinene treatments reduced kindling gain. These results indicate that promotion of epileptogenesis by astrocytes and ECM molecules may be more prominent for kindling acquisition than an increase in excitatory synapses.

5. Conclusion

The results of this study show that in the PTZ kindling epilepsy model, MK-801 and α-pinene attenuate status epilepticus. Furthermore, MK-801 and α-pinene inhibited PTZ-induced astrocyte activation, increased expression of PV protein, and increased ECM molecules. These results indicate that astrocyte activation, and an increase in ECM, are associated with an increase in seizures incidences.

Author contributions

All authors had full access to this study's data and take full responsibility for its integrity and the accuracy of the data analysis. Study concept and design: H.U. and M.O. Data acquisition: H.U., S.S., and Y.T. Data analysis and interpretation: H.U. and S.S. Drafting of the manuscript: H.U. and M.O. Critical revision of the manuscript for important intellectual content: S.M., N.K., K.W., Y.M., and T.I. Statistical analyses: H.U and S.S. Study supervision: M.O. and T.I.

Ethical statement

All procedures related to animal maintenance and experimentation were approved by the Committee for Animal Experiments at the Kawasaki Medical School Advanced Research Center and conformed to the U.S. National Institutes of Health Guide for the Care and Use of Laboratory Animals (NIH Publication No. 80-23, revised in 1996).

Funding sources

This work is supported by a Grant Aid for the Yakumo Foundation for Environmental Science and the Towa Foundation for Food Science & Research.

Data availability statement

All relevant data are within the manuscript.

Conflicts of interest

None.

Acknowledgments

We thank Kawasaki Medical School Central Research Institute for making instruments available to support this study. We would also like to thank Editage (www.editage.jp) for English language editing.

References

Ahmad, A., Husain, A., Mujeeb, M., Khan, S.A., Najmi, A.K., Siddique, N.A., Damanhouri, Z.A., Anwar, F., 2013. A review on therapeutic potential of Nigella sativa: a miracle herb. Asian Pac. J. Trop. Biomed. 3, 337–352.

Ammon-Treiber, S., Grecksch, G., Angelidis, C., Vezyraki, P., Höllt, V., Becker, A., 2007. Pentylenetetrazol-kindling in mice overexpressing heat shock protein 70. Naunyn Schmiedebergs Arch. Pharmacol. 375, 115–121.

Atinga, V., Midala, T.A.S., Timothy, S.Y., Moh'd, A.S., 2015. Evaluation of Mitragyna inermis (wild) leaf extract as an anticonvulsant agent in pentylenetetrazole induced seizures in mice. Adv. Biomed. Pharma. 2, 205–210.

Bandtlow, C.E., Zimmermann, D.R., 2000. Proteoglycans in the developing brain: new conceptual insights for old proteins. Physiol. Rev. 80, 1267–1290.

Bausch, S.B., 2006. Potential roles for hyaluronan and CD44 in kainic acid-induced mossy fiber sprouting in organotypic hippocampal slice cultures. Neuroscience 143, 339–350.

Berardi, N., Pizzorusso, T., Maffei, L., 2004. Extracellular matrix and visual cortical plasticity: freeing the synapse. Neuron 44, 905–908.

Borges, K., Gearing, M., McDermott, D.L., Smith, A.B., Almonte, A.G., Wainer, B.H., Dingledine, R., 2003. Neuronal and glial pathological changes during epileptogenesis in the mouse pilocarpine model. Exp. Neurol. 182, 21–34.

Brückner, G., Brauer, K., Härtig, W., Wolff, J.R., Rickmann, M.J., Derouiche, A., Delpech, B., Girard, N., Oertel, W.H., Reichenbach, A., 1993. Perineuronal nets provide a polyanionic, glia-associated form of microenvironment around certain neurons in many parts of the rat brain. Glia 8, 183–200.

Bygrave, A.M., Masiulis, S., Nicholson, E., Berkemann, M., Barkus, C., Sprengel, R., Harrison, P.J., Kullmann, D.M., Bannerman, D.M., Katzel, D., 2016. Knockout of NMDA-receptors from parvalbumin interneurons sensitizes to schizophrenia-related deficits induced by MK-801. Transl Psychiatry 6, e778.

Caballero, A., Diah, K.C., Tseng, K.Y., 2013. Region-specific upregulation of parvalbumin-, but not calretinin-positive cells in the ventral hippocampus during adolescence. Hippocampus 23 1331-6.

Chan, P.H., Chu, L., Chen, S., 1990. Effects of MK-801 on glutamate-induced swelling of astrocytes in primary cell culture. J. Neurosci. Res. 25 (1), 87–93.

Coan, E.J., Saywood, W., Collingridge, G.L., 1987. MK-801 blocks NMDA receptor-mediated synaptic transmission and long term potentiation in rat hippocampal slices. Neurosci. Lett. 80 (1), 111–114.

Cohen-Gadol, A.A., Pan, J.W., Kim, J.H., Spencer, D.D., Hetherington, H.H., 2004. Mesial temporal lobe epilepsy: a proton magnetic resonance spectroscopy study and a

histopathological analysis. J. Neurosurg. 101, 613–620.
Cremer, C.M., Palomero-Gallagher, N., Bidmon, H.J., Schleicher, A., Speckmann, E.J., Zilles, K., 2009. Pentylenetetrazole-induced seizures affect binding site densities for GABA, glutamate and adenosine receptors in the rat brain. Neuroscience 163 490-9.
da Silva Rivas, Ana Cristina, Lopes, Paula Monteiro, de Azevedo Barros, Mariana Maria, Machado, Danielle Cristina Costa, Alviano, Celuta Sales, Alviano, Daniela Sales, 2012. Biological Activities of α-Pinene and β-Pinene Enantiomers. Molecules. 17 (6), 6305–6316.
de Lanerolle, N.C., Lee, T.S., Spencer, D.D., 2010. Astrocytes and epilepsy. Neurotherapeutics. 7 (4), 424–438.
de Sousa, D.P., Gonçalves, J.C., Quintans-Júnior, L., Cruz, J.S., Araújo, D.A., de Almeida, R.N., 2006. Study of anticonvulsant effect of citronellol, a monoterpene alcohol, in rodents. Neurosci. Lett. 401 (3), 231–235.
Dhir, A., 2012. Pentylenetetrazol (PTZ) kindling model of epilepsy. Curr. Protoc. Neurosci Chapter 9:Unit9.37.
Dingledine, R., McBain, C.J., McNamara, J.O., 1990. Excitatory amino acid receptors in epilepsy. Trends Pharmacol. Sci. 11 334-8.
Dino, M.R., Harroch, S., Hockfield, S., Matthews, R.T., 2006. Monoclonal antibody Cat-315 detects a glycoform of receptor protein tyrosine phosphatase beta/phosphacan early in CNS development that localizes to extrasynaptic sites prior to synapse formation. Neuroscience 142, 1055–1069.
Dityatev, A., 2010. Remodeling of extracellular matrix and epileptogenesis. Epilepsia 51 (Suppl 3), 61–65.
Dorandeu, F., Dhote, F., Barbier, L., Baccus, B., Testylier, G., 2013. Treatment of status epilepticus with ketamine, are we there yet? CNS Neurosci. Ther. 19, 411–427.
Edling, Y., Ingelman-Sundberg, M., Simi, A., 2007. Glutamate activates c-fos in glial cells via a novel mechanism involving the glutamate receptor subtype mGlu5 and the transcriptional repressor DREAM. Glia 55, 328–340.
Eftekhar, F., Yousefzadi, M., Borhani, K., 2004. Antibacterial activity of the essential oil from Ferula gummosa seed. Fitoterapia 75 (7-8), 758–759.
Elger, C.E., Helmstaedter, C., Kurthen, M., 2004. Chronic epilepsy and cognition. Lancet Neurol. 3, 663–672.
Felipe, C.F.B., Albuquerque, A.M.S., de Pontes, J.L.X., de Melo, J.ÍV., Rodrigues, T.C.M.L., de Sousa, A.M.P., Monteiro, ÁB., AEDS, Ribeiro, Lopes, J.P., de Menezes, I.R.A., de Almeida, R.N., 2019. Comparative study of alpha- and beta-pinene effect on PTZ-induced convulsions in mice. Fundam. Clin. Pharmacol. 33, 181–190.
Fisher, R.S., van Emde Boas, W., Blume, W., Elger, C., Genton, P., Lee, P., Engel Jr, J., 2005. Epileptic seizures and epilepsy: definitions proposed by the International League Against Epilepsy (ILAE) and the International Bureau for Epilepsy (IBE). Epilepsia 46 470-2.
Franklin, K., Paxinos, G., 2012. Paxinos and Franklin's the Mouse Brain in Stereotaxic Coordinates, 4th edition. Academic Press.
Frischknecht, R., Heine, M., Perrais, D., Seidenbecher, C.I., Choquet, D., Gundelfinger, E.D., 2009. Brain extracellular matrix affects AMPA receptor lateral mobility and short-term synaptic plasticity. Nat. Neurosci. 12 (7), 897–904.
Gaudet, A.D., Popovich, P.G., 2014. Extracellular matrix regulation of inflammation in the healthy and injured spinal cord. Exp. Neurol. 258, 24–34.
Gray, L., van den Buuse, M., Scarr, E., Dean, B., Hannan, A.J., 2009. Clozapine reverses schizophrenia-related behaviours in the metabotropic glutamate receptor 5 knockout mouse: association with N-methyl-D-aspartic acid receptor up-regulation. Int. J. Neuropsychopharmacol. 12 (1), 45–60.
Guimarães, A.G., Quintans, J.S., Quintans Jr., L.J., 2013. Monoterpenes with analgesic activity–a systematic review. Phytother. Res. 27, 1–15.
Him, A., Ozbek, H., Turel, I., Oner, A.C., 2008. Antinociceptive activity of ALPHA-PINENE and fenchone. Pharmacologyonline 3, 363–369.
Hoffmann, K., Sivukhina, E., Potschka, H., Schachner, M., Löscher, W., Dityatev, A., 2009. Retarded kindling progression in mice deficient in the extracellular matrix glycoprotein tenascin-R. Epilepsia 50, 859–869.
Hussein, A.M., Eldosoky, M., El-Shafey, M., El-Mesery, M., Ali, A.N., Abbas, K.M., Abulseoud, O.A., 2019. Effects of metformin on apoptosis and α-synuclein in a rat model of pentylenetetrazole-induced epilepsy. Can. J. Physiol. Pharmacol. 97, 37–46.
Jarero-Basulto, J.J., Gasca-Martínez, Y., Rivera-Cervantes, M.C., Ureña-Guerrero, M.E., Feria-Velasco, A.I., 2018. Beas-zarate C. Interactions between epilepsy and plasticity. Pharmaceuticals (Basel) 11 (1), 17.
Johnson, K.M., Milner, R., Crocker, S.J., 2015. Extracellular matrix composition determines astrocyte responses to mechanical and inflammatory stimuli. Neurosci. Lett. 600, 104–109.
Kalb, R.G., Hockfield, S., 1994. Electrical activity in the neuromuscular unit can influence the molecular development of motor neurons. Dev. Biol. 162 (2), 539–548.
Kandratavicius, L., Balista, P.A., Lopes-Aguiar, C., Ruggiero, R.N., Umeoka, E.H., Garcia-Cairasco, N., Bueno-Junior, L.S., Leite, J.P., 2014. Animal models of epilepsy: use and limitations. Neuropsychiatr. Dis. Treat. 10, 1693–1705.
Lensjø, K.K., Christensen, A.C., Tennøe, S., Fyhn, M., Hafting, T., 2017. Differential Expression and Cell-Type Specificity of Perineuronal Nets in Hippocampus, Medial Entorhinal Cortex, and Visual Cortex Examined in the Rat and Mouse. eNeuro 4 (3).
Li, B., Wang, L., Sun, Z., Zhou, Y., Shao, D., Zhao, J., Song, Y., Lv, J., Dong, X., Liu, C., Wang, P., Zhang, X., Cui, R., 2014. The anticonvulsant effects of SR 57227 on pentylenetetrazole-induced seizure in mice. PLoS One 9 (4), e93158.
Maeda, N., 2015. Proteoglycans and neuronal migration in the cerebral cortex during development and disease. Front. Neurosci. 9, 98.
Mandhane, S.N., Aavula, K., Rajamannar, T., 2007. Timed pentylenetetrazol infusion test: a comparative analysis with s.c.PTZ and MES models of anticonvulsant screening in mice. Seizure 16, 636–644.
Martin, S., Padilla, E., Ocete, M.A., Galvez, J., Jiménez, J., Zarzuelo, A., 1993. Anti-inflammatory activity of the essential oil of Bupleurum fruticescens. Planta Med. 59 533-6.
Matthews, R.T., Kelly, G.M., Zerillo, C.A., Gray, G., Tiemeyer, M., Hockfield, S., 2002. Aggrecan glycoforms contribute to the molecular heterogeneity of perineuronal nets. J. Neurosci. 22 7536-47.
McRae, P.A., Rocco, M.M., Kelly, G., Brumberg, J.C., Matthews, R.T., 2007. Sensory deprivation alters aggrecan and perineuronal net expression in the mouse barrel cortex. J. Neurosci. 27 (20), 5405–5413.
Mercier, B., Prost, J., Prost, M., 2009. The essential oil of turpentine and its major volatile fraction (alpha- and beta-pinenes): a review. Int. J. Occup. Med. Environ. Health 22, 331–342.
Montes de Oca Balderas, P., Montes de Oca Balderas, H., 2018. Synaptic neuron-astrocyte communication is supported by an order of magnitude analysis of inositol trisphosphate diffusion at the nanoscale in a model of peri-synaptic astrocyte projection. BMC Biophys. 11, 3.
Murray, T.K., Ridley, R.M., 1997. The effect of dizocilpine (MK-801) on conditional discrimination learning in the rat. Behav. Pharmacol. 8 (5), 383–388.
Murray, T.K., Ridley, R.M., Snape, M.F., Cross, A.J., 1995. The effect of dizocilpine (MK-801) on spatial and visual discrimination tasks in the rat. Behav. Pharmacol. 6 (5 & 6), 540–549.
Pahuja, M., Mehla, J., Reeta, K.H., Tripathi, M., Gupta, Y.K., 2013. Effect of Anacyclus pyrethrum on pentylenetetrazole-induced kindling, spatial memory, oxidative stress and rho-kinase II expression in mice. Neurochem. Res. 38, 547–556.
Parsons, C.G., Quack, G., Bresink, I., Baran, L., Przegalinski, E., Kostowski, W., Krzascik, P., Hartmann, S., Danysz, W., 1995. Comparison of the potency, kinetics and voltage-dependency of a series of uncompetitive NMDA receptor antagonists in vitro with anticonvulsive and motor impairment activity in vivo. Neuropharmacology 34, 1239–1258.
Peixoto-Santos, J.E., Kandratavicius, L., Velasco, T.R., Assirati, J.A., Carlotti, C.G., Scandiuzzi, R.C., Salmon, C.E., Santos, A.C., Leite, J.P., 2017. Individual hippocampal subfield assessment indicates that matrix macromolecules and gliosis are key elements for the increased T2 relaxation time seen in temporal lobe epilepsy. Epilepsia 58, 149–159.
Pereira Limberger, R., Mendes Aleixo, A., Fett-Neto, A.G., T Henriques, A., Limberger, R.P., Germano Fett-Neto, A.G.T., 2007. Bioconversion of (+)- and (-)-alpha-pinene to (+)- and (-)-verbenone by plant cell cultures of Psychotria brachyceras and Rauvolfia sellowii. Electron. J. Biotechnol. 10, 500–507.
Perosa, S.R., Porcionatto, M.A., Cukiert, A., Martins, J.R., Passeroti, C.C., Amado, D., Matas, S.L., Nader, H.B., Cavalheiro, E.A., Leite, J.P., Naffah-Mazzacoratti, M.G., 2002. Glycosaminoglycan levels and proteoglycan expression are altered in the hippocampus of patients with mesial temporal lobe epilepsy. Brain Res. Bull. 58, 509–516.
Pizzorusso, T., Medini, P., Berardi, N., Chierzi, S., Fawcett, J.W., Maffei, L., 2002. Reactivation of ocular dominance plasticity in the adult visual cortex. Science 298 (5596), 1248–1251.
Porres-Martínez, M., González-Burgos, E., Carretero, M.E., Gómez-Serranillos, M.P., 2015. Protective properties of Salvia lavandulifolia Vahl. Essential oil against oxidative stress-induced neuronal injury. Food Chem. Toxicol. 80, 154–162.
Rahmati, B., Khalili, M., Roghani, M., Ahghari, P., 2013. Anti-epileptogenic and anti-oxidant effect of Lavandula officinalis aerial part extract against pentylenetetrazol-induced kindling in male mice. J. Ethnopharmacol. 148 152-7.
Scharfman, H.E., 2002. Epilepsy as an example of neural plasticity. Neuroscientist 8, 154–173.
Schmidt, D., Löscher, W., 2005. Drug resistance in epilepsy: putative neurobiologic and clinical mechanisms. Epilepsia 46, 858–877.
Schweizer, M., Streit, W.J., Müller, C.M., 1993. Postnatal development and localization of an N-acetylgalactosamine containing glycoconjugate associated with nonpyramidal neurons in cat visual cortex. J. Comp. Neurol. 329, 313–327.
Seeger, G., Brauer, K., Härtig, W., Brückner, G., 1994. Mapping of perineuronal nets in the rat brain stained by colloidal iron hydroxide histochemistry and lectin cytochemistry. Neuroscience 58, 371–388.
Shapiro, L.A., Wang, L., Ribak, C.E., 2008. Rapid astrocyte and microglial activation following pilocarpine-induced seizures in rats. Epilepsia 49 (Suppl 2), 33–41.
Simonsen, J.L., Ross, W.C.J., 1957. The Triterpenes and their Derivatives : Hydrocarbons, Alcohols, Hydroxy-Aldehydes, Ketones and Hydroxy-Ketones. The Terpenes Vol. 4 University Press, Cambridge.
Singh, H.P., Batish, D.R., Kaur, S., Arora, K., 2006. Kohli RK. Alpha-Pinene inhibits growth and induces oxidative stress in roots. Ann. Bot. 98, : 1261-9.
Skowrońska, K., Obara-Michlewska, M., Zielińska, M., Albrecht, J., 2019. NMDA receptors in astrocytes: in search for roles in Neurotransmission and astrocytic homeostasis. Int. J. Mol. Sci. 20 (2).
Slaker, M., Blacktop, J.M., Sorg, B.A., 2016. Caught in the net: perineuronal nets and addiction. Neural Plast., 7538208.
Souchet, B., Guedj, F., Penke-Verdier, Z., Daubigney, F., Duchon, A., Herault, Y., Bizot, J.C., Janel, N., Créau, N., Delatour, B., Delabar, J.M., 2015. Pharmacological correction of excitation/inhibition imbalance in Down syndrome mouse models. Front. Behav. Neurosci. 9, 267.
Souto-Maior, F.N., Fonsêca, D.V., Salgado, P.R., Monte, L.O., de Sousa, D.P., de Almeida, R.N., 2017. Antinociceptive and anticonvulsant effects of the monoterpene linalool oxide. Pharm. Biol. 55 (1), 63–67.
Squires, R.F., Saederup, E., Crawley, J.N., Skolnick, P., Paul, S.M., 1984. Convulsant potencies of tetrazoles are highly correlated with actions on GABA/benzodiazepine/picrotoxin receptor complexes in brain. Life Sci. 35, 1439–1444.
Sun, Z., Meng, F., Tu, L.X., Sun, L., 2019. Myricetin attenuates the severity of seizures and Neuroapoptosis in pentylenetetrazole kindled mice by regulating the of BDNF-TrkB signaling pathway and modulating matrix metalloproteinase-9 and GABA a. Exp. Ther. Med. 17 (4), 3083–3091.
Svenningsen, A.B., Madsen, K.D., Liljefors, T., Stafford, G.I., van Staden, J., Jäger, A.K.,

2006. Biflavones from Rhus species with affinity for the GABA(A)/benzodiazepine receptor. J. Ethnopharmacol. 103, 276–280.
Tannenberg, R.K., Dodd, P.R., 2009. Cell damage/Excitotoxicity: Excitotoxicity and Neurodegenerative Disease. Encyclopedia of Basic Epilepsy Research XVI. Edited by Philip Schwartzkroin. Elsevier, Oxford, UK, pp. 114–119.
Ueno, H., Suemitsu, S., Okamoto, M., Matsumoto, Y., Ishihara, T., 2017a. Parvalbumin neurons and perineuronal nets in the mouse prefrontal cortex. Neuroscience 343, 115–127.
Ueno, H., Suemitsu, S., Okamoto, M., Matsumoto, Y., Ishihara, T., 2017b. Sensory experience-dependent formation of perineuronal nets and expression of Cat-315 immunoreactive components in the mouse somatosensory cortex. Neuroscience 355161–355174.
Ueno, H., Suemitsu, S., Murakami, S., Kitamura, N., Wani, K., Takahashi, Y., Matsumoto, Y., Okamoto, M., Ishihara, T., 2019a. Alteration of extracellular matrix molecules and perineuronal nets in the Hippocampus of pentylenetetrazol-kindled mice. Neural Plast., 8924634.
Ueno, H., Shimada, A., Suemitsu, S., Murakami, S., Kitamura, N., Wani, K., Matsumoto, Y., Okamoto, M., Ishihara, T., 2019b. Attenuation effects of alpha-pinene inhalation on mice with dizocilpine-induced psychiatric-like behaviour. Evid. Complement. Alternat. Med. 2019, 2745453.
Urbańska, E., Dziki, M., Czuczwar, S.J., Kleinrok, Z., Turski, W.A., 1992. Antiparkinsonian drugs memantine and trihexyphenidyl potentiate the anticonvulsant activity of valproate against maximal electroshock-induced seizures. Neuropharmacology 31, : 1021-6.
Watanabe, Y., Kaida, Y., Fukuhara, S., Takechi, K., Uehara, T., Kamei, C., 2011. Participation of metabotropic glutamate receptors in pentetrazol-induced kindled seizure. Epilepsia 52, 140–150.
Wiese, S., Karus, M., Faissner, A., 2012. Astrocytes as a source for extracellular matrix molecules and cytokines. Front. Pharmacol. 3, 120.
World Health Organization, 2001. Epilepsy: Epidemiology, Aetiology and Prognosis. WHO Factsheet number 165.
Yamada, J., Ohgomori, T., Jinno, S., 2015. Perineuronal nets affect parvalbumin expression in GABAergic neurons of the mouse hippocampus. Eur. J. Neurosci. 41, 368–378.
Yamaguchi, Y., 2000. Lecticans: organizers of the brain extracellular matrix. Cell. Mol. Life Sci. 57, 276–289.
Yang, H., Woo, J., Pae, A.N., Um, M.Y., Cho, N.C., Park, K.D., Yoon, M., Kim, J., Lee, C.J., Cho, S., 2016. α-Pinene, a Major Constituent of Pine Tree Oils, Enhances Non-Rapid Eye Movement Sleep in Mice Through GABAA-benzodiazepine Receptors. Mol. Pharmacol. 90 (5), 530–539.
Ye, Q., Miao, Q.L., 2013. Experience-dependent development of perineuronal nets and chondroitin sulfate proteoglycan receptors in mouse visual cortex. Matrix Biol. 32, 352–363.
Zhou, J.Y., Tang, F.D., Mao, G.G., Bian, R.L., 2004. Effect of alpha-pinene on nuclear translocation of NF-kappa B in THP-1 cells. Acta Pharmacol. Sin. 25 480-4.
Zhou, Y., Li, H.L., Zhao, R., Yang, L.T., Dong, Y., Yue, X., Ma, Y.Y., Wang, Z., Chen, J., Cui, C.L., Yu, A.C., 2010. Astrocytes express N-methyl-D-aspartate receptor subunits in development, ischemia and post-ischemia. Neurochem. Res. 35, 2124–2134.
Zhu, H.L., Wan, J.B., Wang, Y.T., Li, B.C., Xiang, C., He, J., Li, P., 2014. Medicinal compounds with antiepileptic/anticonvulsant activities. Epilepsia. 55 (1), 3–16.